Berry-phase effects in transport through single Jahn-Teller molecules

Maximilian G. Schultz,* Tamara S. Nunner, and Felix von Oppen
Institut für Theoretische Physik, Freie Universität Berlin, 14195 Berlin, Germany
(Received 12 December 2007; published 21 February 2008)

The vibrational modes of Jahn-Teller molecules are affected by a Berry phase that is associated with a conical intersection of the adiabatic potentials. We investigate theoretically the effect of this Berry phase on the electronic transport properties of a single $E\otimes e$ Jahn-Teller molecule when the tunneling electrons continually switch the molecule between a symmetric and a Jahn-Teller distorted charge state. We find that the Berry phase, in conjunction with a spectral trapping mechanism, leads to a current-blockade even in regions outside the Coulomb blockade. The blockade is strongly asymmetric in the gate voltage and induces pronounced negative differential conductance.

DOI: 10.1103/PhysRevB.77.075323 PACS number(s): 73.23.Hk, 71.70.Ej, 81.07.Nb

I. INTRODUCTION

The vision of molecular electronics has stimulated great interest in both the experimental[1–6] and the theoretical[7–14] understanding of electronic transport through single-molecule devices. The coupling of electronic degrees of freedom to few, well-defined molecular vibrations, a property that discriminates transport through single molecules from that through other nanostructures such as quantum dots, sets the stage for observing novel quantum-transport phenomena.[15] One of the simplest and most intensively studied models of such a device is a molecule with a single electronic level and a one-dimensional potential energy surface for the nuclear displacements. This model already gives rise to a large variety of interesting transport phenomena such as vibrational sidebands,[7,8] electron shuttles,[9] Franck-Condon blockade,[10] avalanchelike transport,[10] pair tunneling,[11] and dynamical symmetry breaking.[12] Generalizations of this model to two or more electronic levels have been suggested in order to account for nondegenerate but competing molecular states[13] and for degenerate electronic states on a molecular dimer.[14]

Extensions of the simple molecular model to higher-dimensional potential energy surfaces may seem to be straightforward without yielding qualitatively new physics. This is, however, *not* the case for molecules with symmetry-induced degeneracies of both electronic and vibrational states. For such molecules, the Jahn-Teller effect[16] leads to nontrivial vibrational dynamics, originating in the conical intersections of adiabatic potentials and their associated geometric (Berry) phases. We expect the transport properties to be particularly sensitive to this intriguing dynamics when the tunneling of electrons between molecule and leads switches the molecule between a symmetric and a Jahn-Teller distorted charge state.

In this paper, we investigate the consequences of such a Berry phase for transport through single Jahn-Teller molecules. We focus on the $E\otimes e$ Jahn-Teller effect, for it is the simplest example with a conical intersection of the potential energy surfaces. This type of Jahn-Teller effect occurs for a large variety of triangular (X_3), tetrahedral (ML_4—a transition metal ion M surrounded by a tetrahedron of ligands L), and octahedral molecules or complexes ML_6. We show in Sec. II B that the Berry phase induces a nontrivial selection rule for transitions between vibronic excitations of different molecular charge states. This selection rule, in combination with generic properties of the energy spectrum of the Jahn-Teller molecule, leads to the formation of trapping states in the sequential tunneling limit (Sec. III). The consequences are a current-blockade outside the Coulomb blockade window, asymmetry of the current-voltage characteristics, and strong negative differential conductance (Sec. IV). The appearance of trapping states also strengthens the role of higher-order processes, which introduce a second time scale that is much larger than the scale on which sequential tunneling takes place. The interplay of these two scales renders the details of the tunneling dynamics irrelevant and has a non-negligible effect on the line shape of the differential conductance peaks. We conclude the paper with a discussion of some experimental issues (Sec. V) and an outlook to interesting problems related to electronic transport through Jahn-Teller molecules (Sec. VI).

II. JAHN-TELLER MOLECULE

A. Model

The $E\otimes e$ Jahn-Teller effect generally occurs in molecules where two degenerate electronic states are coupled to two degenerate vibrational modes θ and ε. In the case of an octahedral ML_6 molecule, the relevant electronic states are of $d_{x^2-y^2}$ and $d_{3z^2-r^2}$-types, and the degenerate vibrations correspond to the symmetric oscillations of the ligands as they are pictured in Fig. 1. For definiteness, we assume that without an excess charge on the molecule the degenerate electronic E states are empty.[17] With this choice, the molecular Hamiltonian is[16]

$$H_{E\otimes e} = eV_g n_d + \frac{\hbar\omega}{2}(P_\theta^2 + Q_\theta^2 + P_\varepsilon^2 + Q_\varepsilon^2) + \lambda\hbar\omega(Q_\theta\sigma_x + Q_\varepsilon\sigma_y)n_d. \quad (1)$$

We use a pseudospin notation with Pauli matrices σ_i for the electronic states $|+\rangle$ and $|-\rangle$. The dimensionless strength of the linear coupling of electronic and vibrational degrees of freedom is λ, and ω is the frequency of the vibrational

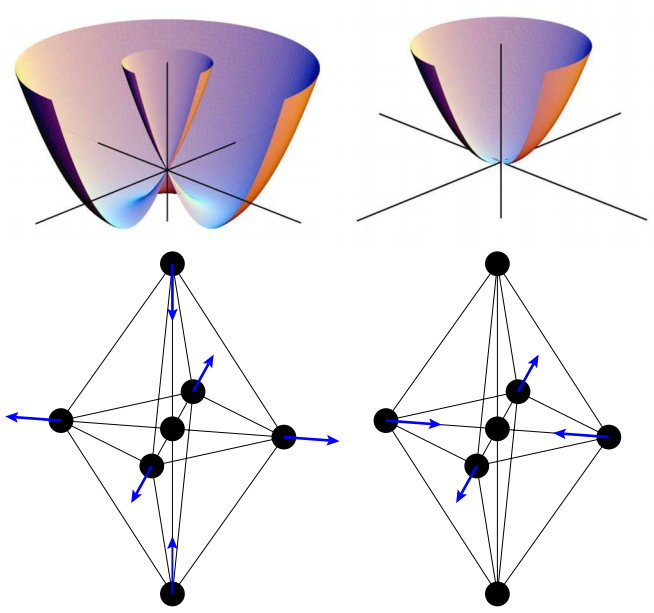

FIG. 1. (Color online) (Top): Adiabatic potentials of the $E\otimes e$ Jahn-Teller distorted (charged) molecule (left) and the undistorted (neutral) molecule (right) as a function of $(Q_\theta, Q\varepsilon)$. (Bottom): Displacement patterns of the degenerate θ and ε vibrations for octahedral ML_6 molecules.

mode with effective mass M and oscillator length $\ell_{\rm osc}=(\hbar/M\omega)^{1/2}$. The dimensionless coordinates Q and momenta P of the normal modes θ and ϵ are measured in units of $\ell_{\rm osc}$. The gate voltage $V_{\rm g}$ tunes the energy of the degenerate electronic levels. $V_{\rm g}=0$ means that for vanishing bias, the molecular levels are degenerate with the Fermi levels of the electrodes. Electronic occupations different from $n_{\rm d}=0$ (neutral molecule) and $n_{\rm d}=1$ (charged molecule) are effectively projected out by assuming a large charging energy U.

The potential surfaces of both charge states are $U(1)$ symmetric in the $(Q_\theta, Q_\varepsilon)$ plane and thus have a conserved angular-momentum quantum number. We shall refer to this angular momentum as a *pseudoangular* momentum to make clear that it does *not* describe rotations in real space but rather a continuous change of the shape of the molecule's distortion. A vibronic state of the neutral molecule is labeled by its *integer* pseudoangular momentum l and radial excitation $n_{\rm r}$. As it is well known from the occupation number representation of the two-dimensional harmonic oscillator, its energy depends on the total number of vibrational quanta no matter in which direction of the oscillator they are excited. The energy manifold $E=(N+1)\hbar\omega$ is N-fold degenerate. In the pseudoangular momentum representation, the degeneracy is reflected in the relation $E_{l,n_{\rm r}}=E_{l+2,n_{\rm r}-1}$, compare Fig. 2(a).

In the charged configuration, on the contrary, with an explicit coupling of vibrations to the pseudospin, it is the *total* pseudoangular momentum $\boldsymbol{j}=\boldsymbol{l}+\frac{1}{2}\boldsymbol{\sigma}$ that is conserved. That the conserved pseudoangular momentum must be a *half-integer* quantity can also be seen by inspection of the adiabatic potentials, which are computed by diagonalizing the potential energy of $H_{E\otimes e}$ for fixed nuclear displacements $(Q_\theta, Q_\varepsilon)$. The two sheets of the $n_{\rm d}=1$ adiabatic potential have, in contrast to the single sheet of the neutral state, a

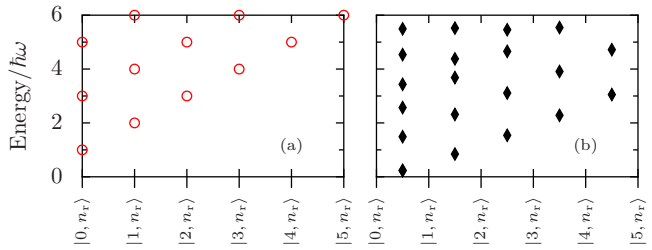

FIG. 2. (Color online) Vibrational spectra (a) of the neutral and (b) of the charged molecule vs pseudoangular momentum. Only energies for positive pseudoangular momenta are shown as the spectra are symmetric under the reflection $l\mapsto -l$.

conical intersection at the origin. Along any loop enclosing the conical intersection, the electronic pseudospin of the adiabatic eigenstates rotates by 2π.[18] The adiabatic eigenstates consequently acquire a Berry phase of π along such closed loops, which must be offset by the vibrational wave function in order to make the full, electronic plus vibrational, wave function single valued. This implies *antiperiodic* boundary conditions for the vibrational wave function and thus *half-integer* pseudoangular momentum j. The spectrum of the charged configuration is plotted in Fig. 2(b) for an intermediate value of the electron-phonon coupling, $\lambda=1$. In contrast to the regularity of the oscillator spectrum, the Jahn-Teller effect lifts the large degeneracy; each state is only doubly degenerate, $E_{j,n_{\rm r}}=E_{-j,n_{\rm r}}$. The Jahn-Teller effect also lowers the ground state energies of each pseudoangular momentum column with respect to the harmonic oscillator energies, which is one of the keys to the current-blockade mechanism discussed in this paper.

The molecular system is coupled to two noninteracting Fermi-gas electrodes labeled by $\alpha=\mathrm{L},\mathrm{R}$. We define electron annihilation operators $c_{\alpha\boldsymbol{k}s}$ for a particle in lead α with wave vector $\boldsymbol{k}$ and spin s, and $d_{\pm,s}$ for a particle on the molecule. The tunneling between the molecule and the electrodes is described by a conventional tunnel Hamiltonian, $H_{\rm T}=t_0\Sigma_{\alpha,\boldsymbol{k},s}c_{\alpha\boldsymbol{k}s}(d^\dagger_{+,s}+d^\dagger_{-,s})+\mathrm{H.c.}$ Jahn-Teller distortions usually occur on a subangstrom scale,[16] which is small compared with the scale on which electronic wave functions fall off. For this reason, we can neglect the dependence of t_0 on the vibrational coordinates. The full Hamiltonian of the single-molecule device is

$$H=H_{E\otimes e}+H_{\rm leads}+H_{\rm T}, \tag{2}$$

where $H_{\rm leads}=\Sigma_\alpha\Sigma_{\boldsymbol{k}s}\varepsilon_{\boldsymbol{k}}c^\dagger_{\alpha\boldsymbol{k}s}c_{\alpha\boldsymbol{k}s}$ is the Hamiltonian of the electrodes. The states of the molecule will be labeled $|n_{\rm d};j,n_{\rm r}\rangle$, $n_{\rm d}$ is the charge on the molecule, j is the pseudoangular momentum (l in the neutral state), and $n_{\rm r}$ enumerates the radial excitations. Our discussion is restricted to the weak tunneling case, where the tunneling induced broadening of the molecular states Γ is small compared with the temperature T, and the predominant transport process is sequential tunneling of electrons. We will only consider a regime of intermediate electron-phonon coupling, where the system is not in the Franck-Condon blockade.[10] The Franck-Condon

blockade effect would not alter the validity of our conclusions but merely complicate the discussion unnecessarily.

B. Selection rule

Any computation of transport properties via an expansion of the system's reduced density matrix in powers of the tunnel Hamiltonian requires the computation of the matrix elements of H_T. An expansion of the Jahn-Teller states $|1;j,n_r\rangle$ in terms of harmonic oscillator eigenstates $|l,n_r'\rangle$ times the two-dimensional electronic manifold $|\pm\rangle$ shows that the electron-phonon interaction due to the $E\otimes e$ Jahn-Teller effect only couples the states $|+\rangle|l,n_r'\rangle$ with the states $|-\rangle|l+1,n_r''\rangle$ of the noninteracting system.[19] The associated half-integer pseudoangular momentum number of the Jahn-Teller state is $j=l+\frac{1}{2}$. The eigenstates of the Jahn-Teller active charge state thus have the general form

$$|1;j,n_r\rangle = \sum_{\tilde{n}_r} \left[A^{jn_r}_{\tilde{n}_r} |+\rangle \left|j-\frac{1}{2},\tilde{n}_r\right\rangle + B^{jn_r}_{\tilde{n}_r} |-\rangle \left|j+\frac{1}{2},\tilde{n}_r\right\rangle \right] \tag{3}$$

for suitable expansion coefficients $A^{jn_r}_{\tilde{n}_r}$ and $B^{jn_r}_{\tilde{n}_r}$. The matrix elements $\langle 0;l,n_r'|H_T|1;j,n_r\rangle$ will therefore vanish unless the pseudoangular momenta fulfill

$$j = l \pm \tfrac{1}{2}. \tag{4}$$

This condition causes many zeros in the tunnel matrix and has a great influence on the transport properties of the device as will be shown in the following sections.

III. CURRENT BLOCKADE

The main result of our paper is a current-blockade effect *outside* the Coulomb blockade diamonds. In certain areas of the (V_g,V_{sd}) plane, the system exhibits "trapping states" that, if populated, lock an excess charge on the molecule and, due to the large charging energy, obstruct any stationary current to flow through the device. These states are vibrational eigenstates of the Jahn-Teller active molecule with pseudoangular momentum $|j|>\frac{1}{2}$. The effect becomes more pronounced for larger pseudoangular momenta. For certain voltage parameters that lie well outside the Coulomb-blockaded region, an electron tunneling from the source electrode can excite the molecule into such states, but it cannot tunnel out toward the drain electrode. The trapping effect itself comes about, because these states become isolated in the tunneling dynamics: either a transition to a neutral target state is forbidden by the selection rule or it is forbidden by conservation of energy.

The implications of this effect for the differential conductance are the formation of structures like those in Fig. 3: a suppression of the stationary current outside the Coulomb-blockaded region. The suppression, however, is not complete; a small stationary current is admitted due to the presence of higher-order processes such as cotunneling, relaxation to thermal equilibrium, or mixing of states by external perturbations, which effectively break the strict selection rule, allowing us to release the system to a vibrational state that can then be left by tunneling. Since these processes are of higher order in t_0, they define a second time scale τ. This time scale, which describes the time that the system will effectively spend in a trapping state, is much larger than the time scale of sequential tunneling, given by H_T, $\tau_0^{-1}:=2\pi\nu t_0^2$, where ν is the density of states in the electrodes.

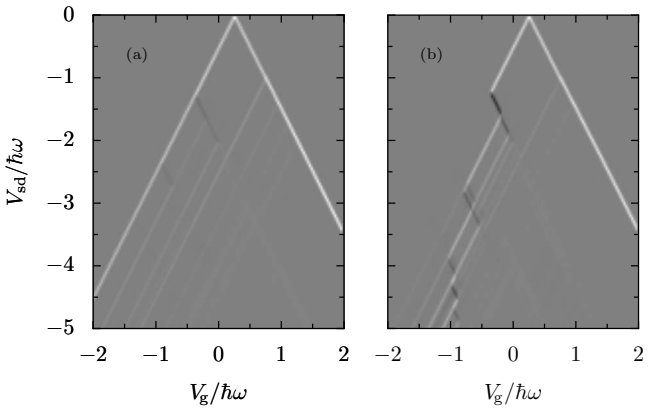

FIG. 3. Differential conductance vs gate voltage V_g and source-drain voltage V_{sd} for $\lambda=1$, $k_BT=0.01\hbar\omega$. (a) $\tau=10\tau_0$; (b) $\tau=5000\tau_0$. White corresponds to positive and black to negative values. Neutral gray is zero differential conductance.

A. Formalism

The technical and formal discussion of the trapping effect is subtle, because due to the high level of degeneracy, one has to employ full master equation dynamics instead of intuitive rate equations for sequential tunneling. The qualitative picture can nonetheless be grasped by rate equations in the pseudoangular momentum basis.

We confine ourselves to the sequential tunneling regime, which means that transitions will only take place between different charge states. We use an expansion of the reduced density matrix ρ in the tunneling Hamiltonian,[8] employ both the Markov and Born approximations, and eventually arrive at a Liouville–von Neumann equation, $\dot{\rho}=-i[H_{leads}+H_{E\otimes e},\rho]+\mathcal{L}\rho$. The operator $\mathcal{L}$ has the well-known Lindblad form for dissipative linear operators and describes the tunneling in second order perturbation theory.[20] Since we are only interested in the stationary transport properties, we can safely neglect those off-diagonal matrix elements of ρ that belong to states of different energies and thus effectively produce a rate-equation dynamics between different energy manifolds. The stationary von Neumann equation reduces with this approximation to $\mathcal{L}\rho=0$. However, since the system under consideration has degenerate states, the equations cannot be further simplified to rate equations for the states $|1;j,n_r\rangle$ and $|0;l,n_r'\rangle$. We do, however, know that the density matrix is a self-adjoint operator and hence admits an eigenbasis in the degenerate subspaces for *each* set of voltage parameters (V_{sd},V_g). In this basis, the von Neumann equation assumes the form of a rate equation, where the rate for a transition between two eigenstates $|\beta\rangle$ and $|\gamma\rangle$ is given by a golden-rule expression

$$M^{\beta\to\gamma} := \frac{2\pi}{\hbar}\nu t_0^2 |\langle\gamma|d_+^\dagger + d_-^\dagger|\beta\rangle|^2, \quad (5)$$

which is of order $\mathcal{O}(H_T^2)$, multiplied by a Fermi function that accounts for the availability of an electron or a hole in the leads. If we want to compute the rates between different energy manifolds in the tunneling problem, we shall consider the unknown, diagonal basis of the degenerate subspaces of ρ at fixed voltages. Let $|\gamma\rangle = \Sigma a_{n_r,l}|l,n_r\rangle$ be one of these states in the neutral configuration and $|\beta\rangle = a_j|j,n_r'\rangle + a_{-j}|-j,n_r'\rangle$ one in the charged configuration. The Franck-Condon factor is

$$|\langle\gamma|H_T|\beta\rangle|^2 = |\sum_{n_r l,\pm j} a^*_{n_r,l} b_j \langle n_r,l|H_T|n_r',j\rangle|^2$$

$$= |\sum_{\pm j} a^*_{n_r,j\pm 1/2} b_j \langle n_r,j \pm \frac{1}{2}|H_T|n_r',j\rangle|^2. \quad (6)$$

The selection rule, which has been shown to be strict in the pseudoangular momentum basis, has thus implications on the transition matrix elements whatever the eigenbasis of ρ is. If the angular momentum of a charged state $|\beta\rangle$ is too large compared with those present in a neutral state $|\gamma\rangle$, a transition may not be allowed. We will show in the next section that such forbidden transitions between energy manifolds are the cause of the current-blockade that we observe analytically and numerically.

B. Trapping states

Considering a sufficiently large bias and a gate voltage that places the ground state of the charged molecule slightly above the Fermi level of the drain electrode, the Fermi functions for relevant excitations are $1-f_{\text{source}}=f_{\text{drain}}\approx 0$, and we only need to discuss the rates for an electron to leave the molecule toward the drain electrode. In this configuration, the system is not in the Coulomb-blockaded region and ought to be conducting. This is, however, *not* the case due to the selection rule [Eq. (4)] and the spectral structure of the molecule. Consider Fig. 4, in which the vibronic spectra of both charge states have been overlaid and shifted by eV_g and $\pm\frac{1}{2}eV_{sd}$ along the energy axis to account for the electronic energies of the charged and neutral states, respectively. Conservation of energy then implies that transitions are energetically possible if the charged target state lies below the neutral initial state in Fig. 4(a) and vice versa in Fig. 4(b), see the figure caption for more details. Take, for example, the state $|\beta\rangle := |1;\frac{5}{2},0\rangle$, the charged state with pseudoangular momentum $j=\frac{5}{2}$, and radial ground state. Once the system occupies this state, it will stay there forever; the electron cannot tunnel to the drain electrode, see Figs. 4 and 5. Conservation of energy requires that any target state has to have less energy than $|\beta\rangle$, so only $l\leqslant 1$ and suitable n are possible. The selection rule [Eq. (4)] only allows the dynamics to connect neighboring columns of Fig. 4. But then all transition rates are zero. The only states that have nonvanishing Franck-Condon factors belong to energy manifolds that due to the specific choice of voltages are out of reach energetically. The state $|\beta\rangle$ is called absorbing or trapping state, that is to say there is no escape rate but yet a finite rate for

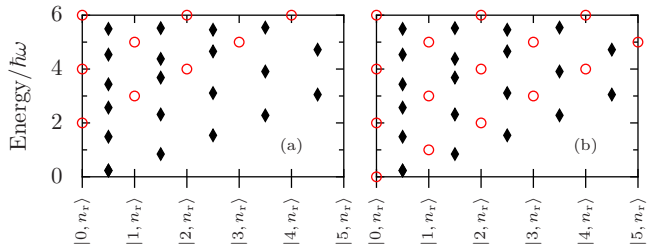

FIG. 4. (Color online) Angular-momentum resolved spectra of the Jahn-Teller molecule ($\lambda=1$) (diamonds) and the neutral molecule (circles). Radial excitations are grouped for each pseudoangular momentum. Panel (a) shows the situation for tunneling at the source electrode and panel (b) the situation at the drain electrode. The chosen parameters are $eV_{sd}=2\hbar\omega$ and $eV_g=-0.5\hbar\omega$. Consider panel (a). An electron can only tunnel from the source electrode and induce the vibronic transition $|0;q\rangle\to|1;q'\rangle$ if the difference in the electronic energy, $\frac{1}{2}eV_{sd}-eV_g$, is larger than the difference in the vibronic energy, $E_{1q'}-E_{0q}$. More precisely, the Fermi function $f\left(e\left(V_g-\frac{1}{2}V_{sd}\right)+E_{1q'}-E_{0q}\right)$ has to be positive. By shifting the neutral spectrum by $\frac{1}{2}eV_{sd}$ and the charged spectrum by eV_g, this relation translates into the intuitive rule that in the diagram the target state of a tunnel process has to lie below the initial state. Energetically allowed transitions are therefore directed downward in the figure. A horizontal transition corresponds to the borderline case of an electron sitting exactly at the Fermi level of the electrode. That conservation of energy has the form of an inequality is due to the filled continuum of states in the Fermi-gas electrode. Panel (b) shows the corresponding energetic situation for sequential tunneling processes at the drain electrode. The presence of trapping states can be seen clearly.

populating the state. The latter of the two properties of $|\beta\rangle$ is easily verified with Fig. 4(a), which shows the shift of the two spectra for tunneling processes from the source electrode. In this configuration there are enough states from which $|\beta\rangle$ can be populated, for instance, the $E=4\hbar\omega$ manifold.

The energy threshold above which a trapping state can be reached from the vibronic ground state of the neutral system marks the onset of the current-blockade in the dI/dV dia-

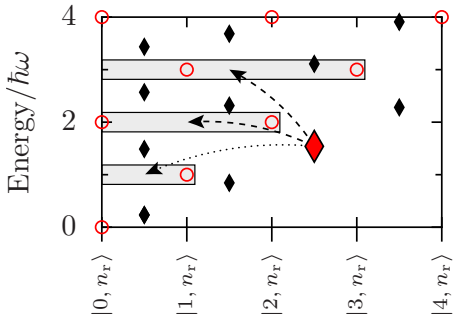

FIG. 5. (Color online) Angular-momentum resolved spectra for tunneling to the drain electrode, $eV_{sd}=2\hbar\omega$ and $eV_g=-0.5\hbar\omega$. The trapping state $|\beta\rangle=|1;\frac{5}{2},0\rangle$ is marked in red. The three nearest energy manifolds of the uncharged system are shaded in gray. The dashed arrows show transitions that are forbidden, because the target manifold's energy is too large. The dotted arrow shows a transition that is forbidden due to the selection rule.

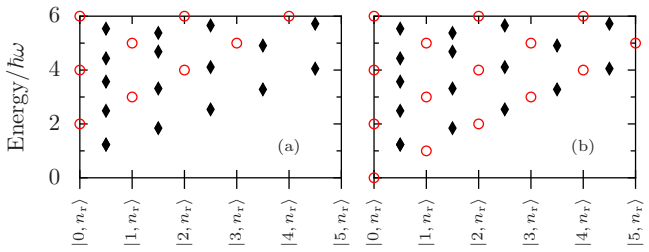

FIG. 6. (Color online) Angular-momentum resolved spectra like in Fig. 4. In this case the Jahn-Teller molecule is placed slightly below the chemical potential of the source electrode. The chosen parameters are $eV_{sd}=2\hbar\omega$ and $eV_g=0.5\hbar\omega$. Contrary to the situation shown in Fig. 4, there are no trapping states.

gram. It can thus cause negative differential conductance peaks, like those in Fig. 3, if the system were conducting below the threshold. Positive differential conductance peaks, on the contrary, can be observed for the energy threshold above which the trapping state acquires a finite escape rate and is no longer trapping. The current-blockade effect, as it has been discussed in the previous paragraph, also produces a significant asymmetry of the dI/dV diagram with respect to V_g. In Fig. 6, we plot the energies of the charged and uncharged states for voltage parameters that place the molecule closely below the Fermi level of the source electrode, that is, for the same V_g as before but with opposite sign. In both processes, tunneling onto and off the molecule, there is no state of the charged system that is isolated due to the selection rule or the spectral distortion. The property of the Jahn-Teller effect to *lower* the energy of the distorted states is the actual reason for this asymmetry. If our Jahn-Teller molecule were such that it was Jahn-Teller active *without* an excess charge and symmetric *with* an additional electron, the situation would be inverted, current-blockade for positive and conducting at negative gate voltage.

IV. RATE EQUATIONS

In the previous paragraphs, we have argued that due to the interplay of the spectral distortion and the selection rule, there are two time scales present in the problem. One describes the tunnel dynamics and is of order $\mathcal{O}(H_T^2)$. The other is due to higher-order processes and is an estimate of how long the system spends in the trapping states. It is thus evident that the precise implementation of the internal dynamics is irrelevant as long as the key ingredients to the separation of time scales, namely, selection rule and spectral distortion, are included.

In this paragraph, we present such a numerical implementation that accounts for the selection rule by employing rate equations in the pseudoangular momentum basis. By doing so, we neglect all coherences between *any* two states in the density matrix, and therefore also those between degenerate states. This will, as we have pointed out before, *not* affect the appearance and structure of the current-blockade, because the effect is independent of the specific form of the eigenbasis of the stationary density matrix. The only error that is introduced by the restriction to rate equations is a quantitative one. The rate equations, on the contrary, allow for a very intuitive and generic treatment of transport problems for systems with spectral distortions and selection rules.

A. Formalism

The occupation probability P_q^n of the molecular eigenstates $|n;q\rangle$ ($n=0,1$ denotes the charge of the molecule, and q is a multiindex for the internal degrees of freedom; Γ is the broadening of the molecular levels due to the coupling to the leads) is governed by the rate equation[8]

$$\dot{P}_q^n = \sum_{n',q'} [P_{q'}^{n'} W_{q'\to q}^{n'\to n} - P_q^n W_{q\to q'}^{n\to n'}] + \gamma_{\rm rel}. \tag{7}$$

The tunnel rates $W_{q\to q'}^{n\to n'}$ are a product of the golden-rule expressions [Eq. (5)] and the Fermi functions of the leads.[8,21] The last term, $\gamma_{\rm rel}=-(1/\tau)[P_q^n - P_q^{\rm eq}\Sigma_{q'}P_{q'}^n]$, describes vibrational relaxation toward the thermal equilibrium distribution $P_q^{\rm eq}$ by higher-order processes not included in the Hamiltonian. By doing so, we effectively implement the aforementioned processes, which release the system from the trapping states. Our results, however, are independent of the details of this implementation. The maximal tunneling rate, τ_0^{-1}, defines the proper time scale on which we measure all times.

The stationary solution of Eq. (7) permits us to compute the stationary current through, say, the left junction,[22]

$$I_{\rm L} = \sum_{qq'} [P_q^0 W_{q\to q';{\rm L}}^{0\to 1} - P_q^1 W_{q\to q';{\rm L}}^{1\to 0}], \tag{8}$$

as a function of the source-drain voltage V_{sd} and the gate voltage V_g. The results for the differential conductance dI/dV_{sd} shown in Fig. 3 for (a) fast and (b) slow vibrational relaxations differ strongly from those obtained for single-mode models.[8] When the molecular orbitals are close to the Fermi energy of the drain electrode (negative V_g in Fig. 3), we find, in accordance with the discussion in Sec. III, an extended region of current suppression outside the Coulomb-blockaded region with large negative differential conductance. No such suppression occurs when the molecular orbitals are close to the chemical potential of the source electrode (positive V_g in Fig. 3), thus rendering dI/dV asymmetric in the gate voltage. The positions of the dI/dV lines that mark the area of the suppressed current in the diagrams are defined by those values of V_{sd} and V_g for which the trapping state is connected to an energy manifold that participates in the transport process. If an increase of the bias voltage generates a finite escape rate for population from the trapping state, that state is no longer absorbing, and a stationary current can flow, hence a line of *positive* differential conductance is observed. In the opposite case, that is, trapping behavior, a line of *negative* differential conductance appears as soon as the principal current carrying states—most often it is sufficient to consider the vibronic ground state of the system—have tunnel rates into the trapping state. Because trapping states are excited vibronic states and intermediate excited states are necessary to access these, there is a certain energy threshold below which a finite current may flow but the trapping state is still out of reach. This threshold will thus be visible as a

negative differential conductance peaks in the dI/dV diagram. Since the trapping states with larger pseudoangular momentum have larger energy thresholds before they can be populated in steady state, the current-blockade mechanism will yield a steplike structure of negative differential conductance peaks and plateaus of suppressed current. These are clearly visible in our numerical results in Fig. 3.

B. Separation of time scales

We further support the irrelevance of the details of the fast, order $\mathcal{O}(H_T^2)$ dynamics by reproducing the positions and line shapes of the peaks in the numerically obtained differential conductance, see Fig. 3, within a simple model. This model only retains the most basic features of the dynamics, namely, the presence of trapping states and the two relevant time scales. Consider a two-level system with a trapping state $|\beta\rangle$ and a state $|\alpha\rangle$ from which the electron can tunnel to the drain electrode, say, the absolute ground state of the charged molecule. The current is given by the inverse of the time τ_{total} the electron spends on the molecule. In our model, this time is the sum of the trapping time τ and the time the electron needs to leave the second, nontrapping state. The rate to leave this latter state is the product of the bare tunneling rate $1/\tau_0$ and the probability $1-f$ to find an empty state of appropriate energy in the drain electrode, where f is this electrode's Fermi function. The typical time for tunneling from $|\alpha\rangle$ out to the leads is thus $\tau_0/(1-f)$ and the stationary current can be estimated as

$$I \propto \frac{1}{\tau_{\text{total}}} = \frac{1}{\tau + \dfrac{\tau_0}{(1-f)}} = \frac{1-f}{(1-f)\tau + \tau_0}. \tag{9}$$

This yields the relation $dI/dV \propto I(\tau I - 1)f/T$. Its consequences for the line shape are twofold. As a purely quantitative effect, the height of the peak in dI/dV decreases with increasing τ. As a qualitative effect, however, the position of the peak is shifted. In a model with just a single time scale, be it a quantum dot or a single-mode molecule, the stationary current through the drain electrode is *only* determined by the Fermi function $1-f(E_{1;q}-E_{0;q'}-\mu_\alpha)$, that is, the probability to find an empty state in the leads with just the energy necessary for the vibrational transition $|0;q'\rangle \leftrightarrow |1;q\rangle$. The maximum of the dI/dV peak is thus located at the bias voltage for which $\mu_\alpha = E_{1;q} - E_{0;q'}$. Within our two-state model, this behavior is recovered for $\tau = 0$ which corresponds to the absence of any trapping effect due to fast relaxation. When trapping is included, and hence τ is finite, the maximum of the differential conductance peak is shifted.

This simple model compares remarkably well to the numerical rate-equation results of the previous section. We focus on a single peak in the dI/dV diagram and study its line shape for different values of the phenomenological relaxation rate τ of Eq. (7). The effect of increasing τ—red to blue curves in Fig. 7(a)—is a reduction of the peak's height and a shift of its position. We can fit the results of our simple model, Eq. (9), to the data in Fig. 7(a), obtaining Fig. 7(b). Comparing the fit values for τ with the parameters of the numerical simulation, see Fig. 8, we can see how well this simplified model describes the interplay of the two time scales. The only deviations occur when both time scales are of comparable magnitude, $\tau = \mathcal{O}(\tau_0)$. In contrast, for a sufficiently large separation of time scales, the agreement is nearly perfect. This backs our general considerations of Sec. III, where we have argued that the observed phenomena are of a generic nature.

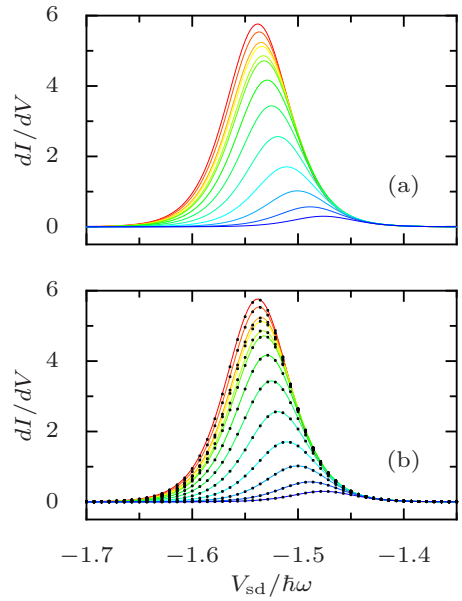

FIG. 7. (Color online) Positive differential conduction peak at the Coulomb blockade, $V_g = -0.5\hbar\omega$, for different values of the relaxation time τ (a) and fit with the simplified model, dots in (b). The red curves, that is, the large, centered peaks have small, and the blue ones, damped and shifted to lower V_{sd}, very large τ.

The predominant features of electronic transport through a single Jahn-Teller molecule are determined by three properties of the system: the spectral distortion and the selection rule fix the position of the peaks in the differential conductivity; their heights are determined by the Franck-Condon matrix elements. Finally, higher-order processes introduce a second, larger time scale, which eventually determines the exact line shape.

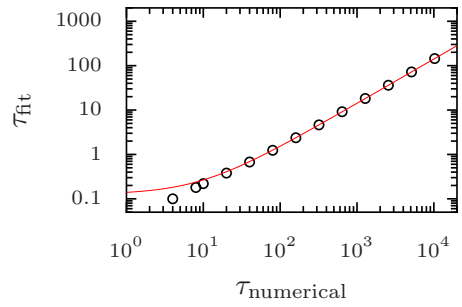

FIG. 8. (Color online) Fit τ values of the simplified model (dots) and its application to Fig. 7 vs the numerical values used in the actual simulation. The curve is a linear fit to these values, $\tau_{\text{fit}} \propto \tau_{\text{numerical}}$, showing the validity of the simplified approach in the regime of strong separation of the time scales.

V. EXPERIMENTAL ISSUES

We finally discuss several experimental issues. Placing a Jahn-Teller molecule between two biased electrodes exposes it to a potentially large electric field. For a semiconductor quantum dot, weak coupling and good screening imply that the potential drop is concentrated in the contact regions between the electrodes and the dot.[23] For a single molecule, however, this is less obvious. Thus, the electric field may lift the electronic degeneracy by the Stark effect and mix the vibronic levels by breaking the rotational symmetry of the adiabatic potential.

To estimate the mixing of vibronic levels, we note that the relevant vibrational modes θ and ε do not possess a dipole moment and are therefore unaffected by the electric field unless anharmonic mode mixing becomes relevant when other, "dipole-active" modes are strongly displaced. One readily estimates, however, that for relevant electric fields (corresponding to voltage drops of the order of $\hbar\omega$) the typical displacements of dipole-active vibrational modes are small compared with their oscillator length ℓ_{osc}, so that no anharmonic effects are expected. Assuming that the dipole moment is of order ex, where x is the displacement of the dipole-active mode, we obtain a displacement $x \sim eE/M\omega^2 \sim \ell_{\mathrm{osc}}^2/\delta \ll \ell_{\mathrm{osc}}$. The length δ is of the order of the size of the molecular junction. We also note that the electric field does not directly couple the two electronic levels as both are d orbitals. The Stark shift is therefore quadratic in the electric field, and we estimate that it is several orders of magnitude smaller than the vibrational frequency.

The coupling of the Jahn-Teller molecule to fermionic reservoirs, the electronic leads, may also introduce external perturbations that are able to break the symmetries of the system on which our approach relies so heavily. If the perturbation is too strong, for example, the degeneracy of the vibrational modes θ and ε is lifted and the energies are shifted by a large amount. The Jahn-Teller effect is then no longer of $E\otimes e$ but rather of $E\otimes(b_1+b_2)$ type. A selection rule like the one used in this paper is not available in such a model, and the current-blockade would not be visible. If, however, the perturbation is only small compared with the tunnel coupling, the mixing of the states induced by the perturbation is able to introduce a second time scale $\tau \gg \tau_0$ into the problem. As we have discussed in the previous paragraphs, the presence of two widely separated time scales only shifts the positions and alters the shape of the differential conductance peaks, no matter what the detailed physics behind the phenomenology of the conduction peaks are.

VI. CONCLUSIONS

We have shown that symmetry-induced degeneracies of electronic and vibrational modes can lead to new transport phenomena in single-molecule junctions. When the molecular junction consists of, say, an octahedral complex with an $E\otimes e$ Jahn-Teller effect, a combination of Berry-phase effects and a spectral trapping mechanism results in a nontrivial current-blockade, even for parameters where the Coulomb blockade is lifted. It is evident from the physics of this blockade mechanism developed in this paper that it is associated with strongly enhanced shot noise of the current.[24] We have also shown that the mechanism is quite generic and that the introduction of a second time scale to the problem, for example, by higher-order relaxation processes, cotunneling, or external perturbations, has only quantitative effects on our results.

The good agreement of the numerical results of our effective rate model with the general consideration of Sec. III shows that the current-blockade that has been found in this context is a generic effect of systems with selection rules and spectral distortions. Nowack and Wegewijs[13] find a related current-blockade effect in systems where the strong spectral distortion alone damps certain Franck-Condon matrix elements. This is, however, no selection rule that derives from symmetries like in this paper; it rather stems from the almost vanishing overlap of displaced oscillator wave functions.

Our discussion of Jahn-Teller molecules raises several interesting questions. The most important question concerns a complete understanding of the role of coherences between degenerate states and their implications for the transport properties of the system. What are the experimentally measurable quantities that are influenced by nondiagonal elements of the density matrix? When is a reduction to rate equations allowed?

ACKNOWLEDGMENTS

This work was supported in part by SPP 1243 of the Deutsche Forschungsgemeinschaft as well as SFB 658.

*mschultz@physik.fu-berlin.de

[1] H. Park, J. Park, A. K. L. Lim, E. H. Anderson, A. P. Alvisatos, and P. L. McEuen, Nature (London) **407**, 57 (2000).

[2] R. H. M. Smit, Y. Noat, C. Untiedt, N. D. Land, M. C. van Hemert, and J. M. van Ruitenbeek, Nature (London) **419**, 906 (2002).

[3] J. Park, A. N. Pasupathy, J. I. Goldsmith, C. Chang, Y. Yaish, J. R. Petta, M. Rinkoski, J. P. Sethna, H. D. Abruña, P. L. McEuen, and D. C. Ralph, Nature (London) **417**, 722 (2002).

[4] H. B. Heersche, Z. de Groot, J. A. Folk, H. S. J van der Zant, C. Romeike, M. R. Wegewijs, L. Zobbi, D. Barreca, E. Tondello, and A. Cornia, Phys. Rev. Lett. **96**, 206801 (2006).

[5] T. Dadosh, Y. Gordin, R. Krahne, I. Khivrich, D. Mahalu, V. Freydman, J. Sperling, A. Yacoby, and I. Bar-Joseph, Nature (London) **436**, 677 (2005).

[6] L. H. Yu, Z. K. Keane, J. W. Ciszek, L. Cheng, J. M. Tour, T. Baruah, M. R. Pederson, and D. Natelson, Phys. Rev. Lett. **95**, 256803 (2005).

[7] S. Braig and K. Flensberg, Phys. Rev. B **68**, 205324 (2003).

[8] A. Mitra, I. Aleiner, and A. J. Millis, Phys. Rev. B **69**, 245302

(2004).
[9] L. Y. Gorelik, A. Isacsson, M. V. Voinova, B. Kasemo, R. I. Shekhter, and M. Jonson, Phys. Rev. Lett. **80**, 4526 (1998).
[10] J. Koch and F. von Oppen, Phys. Rev. Lett. **94**, 206804 (2005).
[11] J. Koch, M. E. Raikh, and F. von Oppen, Phys. Rev. Lett. **96**, 056803 (2006).
[12] A. Donarini, M. Grifoni, and K. Richter, Phys. Rev. Lett. **97**, 166801 (2006).
[13] K. C. Nowack and M. R. Wegewijs, New J. Phys. **7**, 239 (2005).
[14] G. A. Kaat and K. Flensberg, Phys. Rev. B **71**, 155408 (2005).
[15] For a recent review, see M. Galperin, M. A. Ratner, and A. Nitzan, J. Phys.: Condens. Matter **19**, 103201 (2007).
[16] I. B. Bersuker, *The Jahn-Teller Effect* (Cambridge University Press, Cambridge, 2006).
[17] Our results are independent of this choice as long as the tunneling electron switches the molecule between its Jahn-Teller distorted and symmetric states.
[18] M. V. Berry, Proc. R. Soc. London, Ser. A **392**, 45 (1984).
[19] H. C. Longuet-Higgins, U. Öpik, M. H. L. Pryce, and R. A. Sachs, Proc. R. Soc. London, Ser. A **244**, 1 (1958).
[20] K. Blum, *Density Matrix Theory and Applications* (Plenum, New York, 1981).
[21] J. Koch, F. von Oppen, Y. Oreg, and E. Sela, Phys. Rev. B **70**, 195107 (2004).
[22] The index L on the rates indicates that only this lead's Fermi function is used for the computation of the rate.
[23] Y. Xue and M. A. Ratner, Phys. Rev. B **68**, 115406 (2003).
[24] M. G. Schultz, T. S. Nunner, and F. von Oppen (unpublished).